Identifying a new particle with jet substructures

Lim, Sung Hak

Theory Center, KEK, Japan

Higgs Coupling 2017

Nov. 2017

BSM and Heavy Scalar

- Many theories beyond the Standard model (SUSY, composite Higgs...) could have extended Higgs sector with particles having masses more than $\mathcal{O}(1)$ TeV to make model compatible with the current observation about the Higgs boson.
  - Example: heavy Higgs boson in MSSM
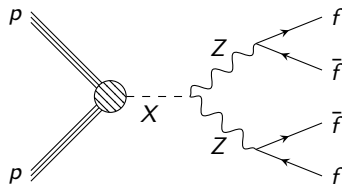- mass eigenstates: h^0 , H^0, $H^{\pm}$ and A^0

$$
m_{H^{\pm}}^2 = m_{A^0}^2 + m_W^2 \tag{1}
$$
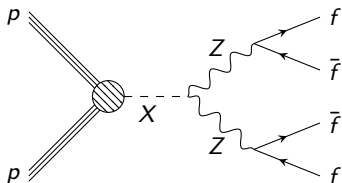
$$
m_{h^0,H^0}^2 = \frac{1}{2}\left(m_{A^0}^2 + m_Z^2 \mp \sqrt{(m_{A^0}^2 - m_Z^2)^2 + 4m_Z^2 m_{A^0}^2 sin^2 2\beta}\right) \tag{2}
$$

- In a limit $m_{A^0} \gg m_Z$ (decoupling limit),

$$
m_Z \sim m_{h^0} \ll m_{H^0} \sim m_{H^{\pm}} \sim m_{A^0} \tag{3}
$$

- h^0 behaves like the Higgs boson in the Standard model, while other heavy scaler lives in higher energy scale.
- One interesting channel for identifying heavy Higgs bosons is ZZ channel.

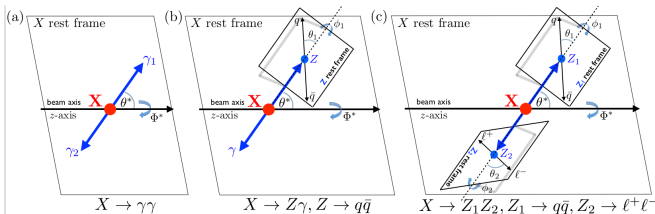## Characteristics of $X \rightarrow ZZ$ channel

Introduction
○●○○○○

Quantum interference and angular correlations
○○○

Phase space reduction and merged jet
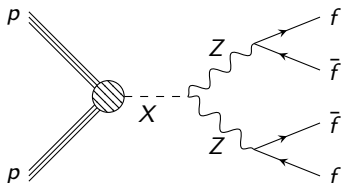○○○○○

Conclusion
○

Characteristics of $X \to ZZ$ channel

- Good: this channel is fully capable of determining spin and CP nature of X.

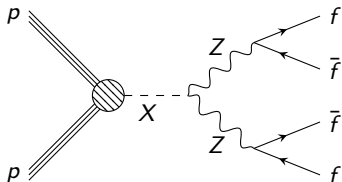Characteristics of $X \to ZZ$ channel
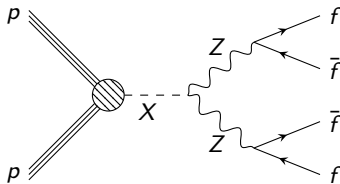
- Good: this channel is fully capable of determining spin and CP nature of X.
  - $\gamma\gamma$: polarization-blind, we cannot fully determine spin and CP of X.
  - ZZ: we can get additional polarization information of Z boson from differential distribution of Fermions.

Characteristics of $X \rightarrow ZZ$ channel

- Good: this channel is fully capable of determining spin and CP nature of X.
- Problem: (For heavy X, $m_X \gg m_Z$) Z boson is boosted, and two Fermions (especially quarks) are often too close and identified as a single large cluster.

3 / 16

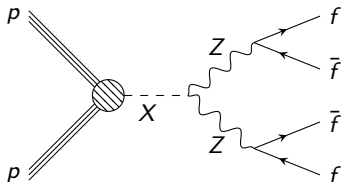## Characteristics of $X \rightarrow ZZ$ channel

- Good: this channel is fully capable of determining spin and CP nature of X.
- Problem: (For heavy X, $m_X \gg m_Z$) Z boson is boosted, and two Fermions (especially quarks) are often too close and identified as a single large cluster.
    - In order to use full potential of ZZ channel, We should resolve the cluster.
    - We will see that the jet substructure technique can be used for resolving the cluster and effectively and selecting effective region for discriminating spin and CP of X.

3 / 16

Characteristics of $X \to ZZ$ channel

- Good: this channel is fully capable of determining spin and CP nature of X.
- Problem: (For heavy X, $m_X \gg m_Z$) Z boson is boosted, and two Fermions (especially quarks) are often too close and identified as a single large cluster.
    - In order to use full potential of ZZ channel, We should resolve the cluster.
    - We will see that the jet substructure technique can be used for resolving the cluster and effectively and selecting effective region for discriminating spin and CP of X.
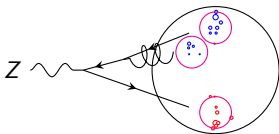- One simple example: mass-drop tagger
  (J. M. Butterworth, A. R. Davison, M. Rubin and G. P. Salam, arXiv:0802.2470)

3 / 16

Identifying boosted $Z \to q\bar{q}$ with merged jet

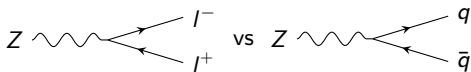- We can identify momenta of two prong subjets by the mass-drop tagger.

- Merged jet identification: Cambridge-Aachen algorithm with large radius
- Jet substructure for identifying $q\bar{q}$
    - Rewind Cambridge-Aachen jet clustering to access clustering sequence in angular order
    - mass-drop and filtering: look for clustering point with mass drop

$$m_{j_1} < \mu m_j \tag{4}$$
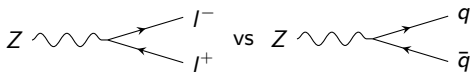
    and splitting, i.e. symmetric p_T condition

$$\frac{\min(p_{T,j_1}^2, p_{T,j_2}^2)}{m_j^2}(\Delta R_{j_1 j_2})^2 > y_{\text{cut}} \tag{5}$$

    - Output: corresponding clustering distance, which is angular scale, can be used for identifying subjet which can resemble $q\bar{q}$.

- This subjet momenta can be used for identifying CP state of S!

Introduction
○○○●○○

Quantum interference and angular correlations
○○○

Phase space reduction and merged jet
○○○○○

Conclusion
○

boosted Z boson to leptons vs quarks

Z ⟶ l^- l^+ vs Z ⟶ q $\bar{q}$

- advantages

- disadvantages

boosted Z boson to leptons vs quarks

$$Z \sim\!\!\sim\!\!\sim\!\!< \begin{array}{l} l^- \\ l^+ \end{array} \quad \text{vs} \quad Z \sim\!\!\sim\!\!\sim\!\!< \begin{array}{l} q \\ \bar{q} \end{array}$$

- advantages

- disadvantages

  - more events!

$$
\begin{aligned}
BR(Z \to e^+ e^-) &= 3.363\% \\
BR(Z \to \mu^+ \mu^-) &= 3.366\% \\
BR(Z \to \text{invisible}) &= 20.00\% \\
BR(Z \to \text{hadrons}) &= 69.91\%
\end{aligned}
$$

boosted Z boson to leptons vs quarks

$$Z \sim\!\!\!\!\!\!\!\!<\begin{array}{c} l^- \\ l^+ \end{array} \quad \text{vs} \quad Z \sim\!\!\!\!\!\!\!\!<\begin{array}{c} q \\ \bar{q} \end{array}$$

- advantages

  - more events!

$$
\begin{array}{rcl}
BR(Z \to e^+ e^-) & = & 3.363\% \\
BR(Z \to \mu^+ \mu^-) & = & 3.366\% \\
BR(Z \to \text{invisible}) & = & 20.00\% \\
BR(Z \to \text{hadrons}) & = & 69.91\%
\end{array}
$$

- disadvantages

  - hard to resolve two close quarks.

5 / 16

boosted Z boson to leptons vs quarks

$$Z \sim\!\!\!\!\wedge\!\!\!\!\wedge\!\!\!\!< \begin{array}{c} l^- \\ l^+ \end{array} \quad \text{vs} \quad Z \sim\!\!\!\!\wedge\!\!\!\!\wedge\!\!\!\!< \begin{array}{c} q \\ \bar{q} \end{array}$$
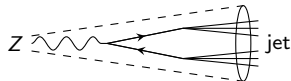
- advantages

    - more events!

$$
\begin{aligned}
BR(Z \to e^+ e^-) &= 3.363\% \\
BR(Z \to \mu^+ \mu^-) &= 3.366\% \\
BR(Z \to \text{invisible}) &= 20.00\% \\
BR(Z \to \text{hadrons}) &= 69.91\%
\end{aligned}
$$

- disadvantages

    - hard to resolve two close quarks.

- contamination from nearby QCD activity
    - underlying events
    - final state radiations
    - pile-ups
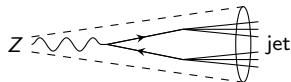
boosted Z boson to leptons vs quarks

$$Z \sim\!\!\!\!\!\!<\begin{matrix} l^- \\ l^+ \end{matrix} \text{ vs } Z \sim\!\!\!\!\!\!<\begin{matrix} q \\ \bar{q} \end{matrix}$$

- advantages

    - more events!

$$BR(Z \to e^+ e^-) = 3.363\%$$
$$BR(Z \to \mu^+ \mu^-) = 3.366\%$$
$$BR(Z \to \text{invisible}) = 20.00\%$$
$$BR(Z \to \text{hadrons}) = 69.91\%$$

- disadvantages

    - hard to resolve two close quarks.

$$Z \sim\!\!\!\!\!\!<\!\!\!\equiv\!\!\!\quad \text{jet}$$

    - contamination from nearby QCD activity
        - underlying events
        - final state radiations
        - pile-ups
        - Many background events..
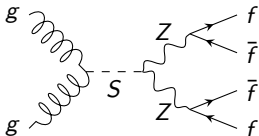
5 / 16

Summing up advantages and disadvantages
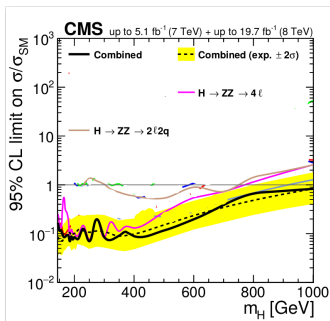
- $ZZ \rightarrow 2\ell2q$ having same sensitivity level to the $ZZ \rightarrow 4\ell$ in high mass resonance searches. [CMS-CR-2015-045]
- We can play similarly to 4*l* channel to identifying quantum state of heavy scalar!
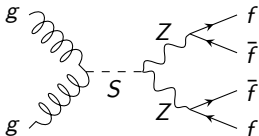
We particularly considered scalar resonances in CP eigenstate.

Benchmark point

We particularly considered scalar resonances in CP eigenstate.

$$\mathcal{L}_{0^{++}} \;\; = \;\; \frac{c_{gg}}{\Lambda} S G_{\mu\nu} G^{\mu\nu} + \frac{c_{ZZ}}{\Lambda} S Z_{\mu\nu} Z^{\mu\nu}$$
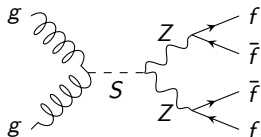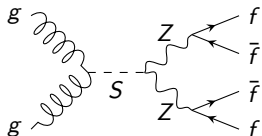
Benchmark point

We particularly considered scalar resonances in CP eigenstate.

$$\mathcal{L}_{0^{++}} = \frac{c_{gg}}{\Lambda} S G_{\mu\nu} G^{\mu\nu} + \frac{c_{ZZ}}{\Lambda} S Z_{\mu\nu} Z^{\mu\nu}$$
$$\mathcal{L}_{0^{-+}} = \frac{c_{gg}}{\Lambda} S G_{\mu\nu} \tilde{G}^{\mu\nu} + \frac{c_{ZZ}}{\Lambda} S Z_{\mu\nu} \tilde{Z}^{\mu\nu}$$

| Introduction | Quantum interference and angular correlations | Phase space reduction and merged jet | Conclusion |
| 000000● | 000 | 00000 | 0 |

Benchmark point

benchmark points $\quad r_M \quad \Delta R \gtrsim$

We particularly considered scalar resonances in CP eigenstate.

$$\mathcal{L}_{0^{++}} = \frac{c_{gg}}{\Lambda} S G_{\mu\nu} G^{\mu\nu} + \frac{c_{ZZ}}{\Lambda} S Z_{\mu\nu} Z^{\mu\nu}$$
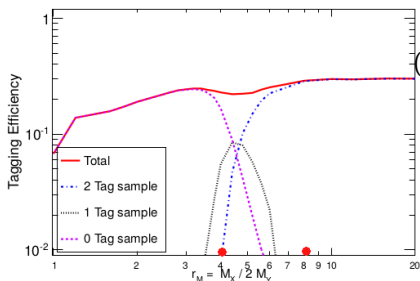
$$\mathcal{L}_{0^{-+}} = \frac{c_{gg}}{\Lambda} S G_{\mu\nu} \tilde{G}^{\mu\nu} + \frac{c_{ZZ}}{\Lambda} S Z_{\mu\nu} \tilde{Z}^{\mu\nu}$$

Benchmark point

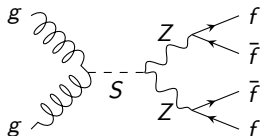| benchmark points	r_M	$\Delta R \gtrsim$
$m_S = 750\,\mathrm{GeV}$	4.1	0.5

$$r_M = \frac{m_S}{2m_Z}$$

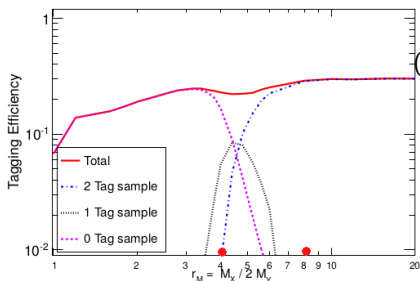$$(\Delta R) = \sqrt{(\Delta\eta)^2 + (\Delta\phi)^2} \gtrsim \frac{4m_Z}{\sqrt{m_S^2 - 4m_Z^2}}$$

M. Gouzevitch, et al., arXiv:1303.6636

Benchmark point

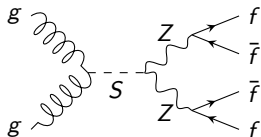| benchmark points	r_M	$\Delta R \gtrsim$
$m_S = 750\,\mathrm{GeV}$	4.1	0.5
$m_S = 1500\,\mathrm{GeV}$	8.2	0.25

$$r_M = \frac{m_S}{2m_Z}$$

$$(\Delta R) = \sqrt{(\Delta\eta)^2 + (\Delta\phi)^2} \gtrsim \frac{4m_Z}{\sqrt{m_S^2 - 4m_Z^2}}$$

M. Gouzevitch, et al., arXiv:1303.6636

7 / 16

Benchmark point

benchmark points	r_M	$\Delta R \gtrsim$
$m_S = 750\,\mathrm{GeV}$	4.1	0.5
$m_S = 1500\,\mathrm{GeV}$	8.2	0.25

We particularly considered scalar resonances in CP eigenstate.

$$\mathcal{L}_{0^{++}} = \frac{c_{gg}}{\Lambda} S G_{\mu\nu} G^{\mu\nu} + \frac{c_{ZZ}}{\Lambda} S Z_{\mu\nu} Z^{\mu\nu}$$

$$\mathcal{L}_{0^{-+}} = \frac{c_{gg}}{\Lambda} S G_{\mu\nu} \tilde{G}^{\mu\nu} + \frac{c_{ZZ}}{\Lambda} S Z_{\mu\nu} \tilde{Z}^{\mu\nu}$$
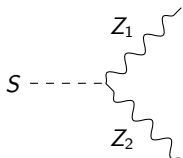
We performed statistical analysis with Monte Carlo simulated event together with detector simulations.

Quantum interference and angular correlations

- In order to identify spin and CP of S, angular correlation between resonances are the key signatures.

Quantum interference and angular correlations

- In order to identify spin and CP of S, angular correlation between resonances are the key signatures.
- In particular, angular correlation between two Z boson system is especially useful for identifying CP of S, because $\mathcal{L}_{0\pm+}$ produce two Z boson in entangled helicity eigenstate ($\epsilon_\pm$).

$$
S \text{-----} \begin{cases} Z_1 \\ \\ Z_2 \end{cases} \propto \begin{cases} \epsilon_+^{*\mu}(Z_1)\epsilon_+^{*\nu}(Z_2) + \epsilon_-^{*\mu}(Z_1)\epsilon_-^{*\nu}(Z_2) & S \text{ in } \mathcal{L}_{0^{++}} \\ \epsilon_+^{*\mu}(Z_1)\epsilon_+^{*\nu}(Z_2) - \epsilon_-^{*\mu}(Z_1)\epsilon_-^{*\nu}(Z_2) & S \text{ in } \mathcal{L}_{0^{-+}} \end{cases}
$$

($m_X \gg m_Z$ is assumed)

8 / 16

Quantum interference and angular correlations

- In order to identify spin and CP of S, angular correlation between resonances are the key signatures.

- In particular, angular correlation between two Z boson system is especially useful for identifying CP of S, because $\mathcal{L}_{0\pm+}$ produce two Z boson in entangled helicity eigenstate ($\epsilon_{\pm}$).

$$
S \, \text{-----} \quad
\begin{matrix}
Z_1 \\
\\
Z_2
\end{matrix}
\quad \propto
\begin{cases}
\epsilon_+^{*\mu}(Z_1)\epsilon_+^{*\nu}(Z_2) + \epsilon_-^{*\mu}(Z_1)\epsilon_-^{*\nu}(Z_2) & S \text{ in } \mathcal{L}_{0^{++}} \\
\epsilon_+^{*\mu}(Z_1)\epsilon_+^{*\nu}(Z_2) - \epsilon_-^{*\mu}(Z_1)\epsilon_-^{*\nu}(Z_2) & S \text{ in } \mathcal{L}_{0^{-+}}
\end{cases}
$$

- Angular correlation arise from interference between helicity eigenstates.
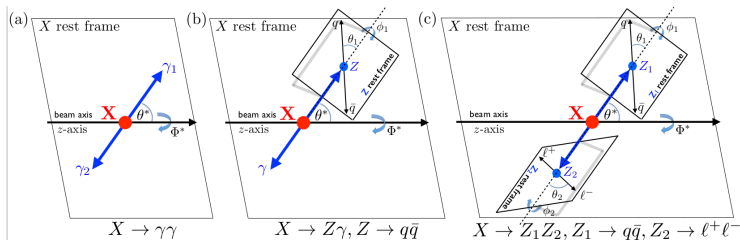
Quantum interference and angular correlations
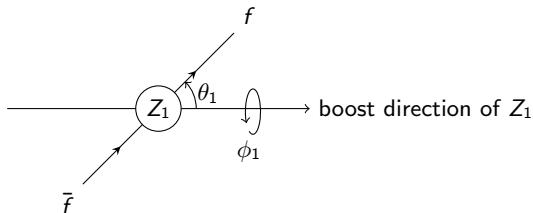
- Interference term leaves an azimuthal phase factor so it can be captured by angular correlations.

$$\sum_{\text{spin of } f, \bar{f}} \left(\epsilon_\pm \sim\!\!\!\!\sim\!\!\!\!\sim \cdot \sim\!\!\!\!\sim\!\!\!\!\sim \epsilon_\mp^* \right) \propto -\sin^2\theta_1 e^{\pm 2i\phi_1}$$
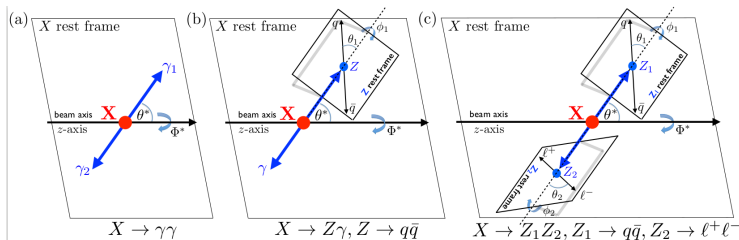
- Interference term is maximized when $f\bar{f}$ are emitted to transverse direction. This is consequence of the Stern-Gerlach experiment, $[S_z, S_x] \neq 0$.

9 / 16

Introduction
000000
Quantum interference and angular correlations
000●
Phase space reduction and merged jet
00000
Conclusion
0

Quantum interference and angular correlations

- As a result $\phi = \phi_1 - \phi_2$, which is the angle between two Z boson decay plane, can discriminate CP of S.

Quantum interference and angular correlations

(a) X rest frame, $X \to \gamma\gamma$

(b) X rest frame, $X \to Z\gamma, Z \to q\bar{q}$

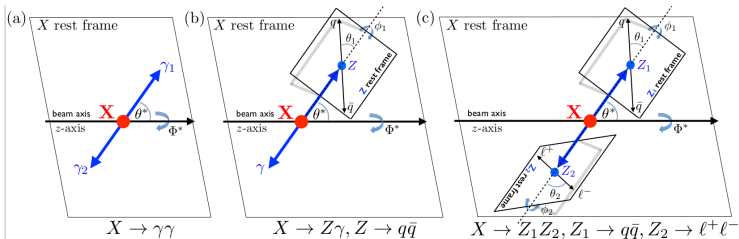(c) X rest frame, $X \to Z_1 Z_2, Z_1 \to q\bar{q}, Z_2 \to \ell^+\ell^-$

- As a result $\phi = \phi_1 - \phi_2$, which is the angle between two Z boson decay plane, can discriminate CP of S.

$$\sum_{\text{spin of } q, \bar{q}, \ell^-, \ell^-} \left| \begin{matrix} \end{matrix} \right|^2 \propto \begin{array}{c} (1 + \cos^2\theta_1)(1 + \cos^2\theta_2) \\ \pm \sin^2\theta_1 \sin^2\theta_2 \cos 2\phi \end{array}$$

$$\text{for } S \text{ in } \mathcal{L}_{0\pm+}, \quad m_S \gg m_Z .$$

Introduction
000000
Quantum interference and angular correlations
00●
Phase space reduction and merged jet
00000
Conclusion
0

Quantum interference and angular correlations

(a) $X \to \gamma\gamma$ (b) $X \to Z\gamma, Z \to q\bar{q}$ (c) $X \to Z_1 Z_2, Z_1 \to q\bar{q}, Z_2 \to \ell^+\ell^-$

- As a result $\phi = \phi_1 - \phi_2$, which is the angle between two Z boson decay plane, can discriminate CP of S.

$$\sum_{\text{spin of } q, \bar{q}, \ell^-, \ell^-} \left| \text{---}\langle\!\langle \right|^2 \propto \begin{array}{c} (1 + \cos^2\theta_1)(1 + \cos^2\theta_2) \\ \pm \sin^2\theta_1 \sin^2\theta_2 \cos 2\phi \\[2mm] \text{for } S \text{ in } \mathcal{L}_{0\pm+}, \quad m_S \gg m_Z . \end{array}$$

- This ME is prportional to likelihoods of $0^{\pm+}$ hypotheses. Therefore, how we select two Fermions from Z is also important to gain maximum sensitivity for signal disambiguation.

Introduction
000000

Quantum interference and angular correlations
000

Phase space reduction and merged jet
●0000

Conclusion
○

Relativistic Aberration and angular separation of $f\bar{f}$
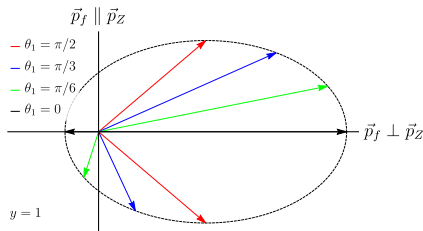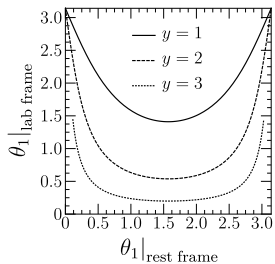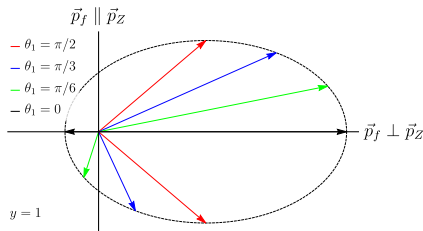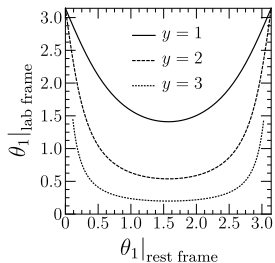
When we try to capture two $q\bar{q}$ by a single merged jet, Fermions emitted transverse direction from the boost direction of Z boson will be captured more than the longitudinal direction.

Relativistic Aberration and angular separation of $f\bar{f}$

When we try to capture two $q\bar{q}$ by a single merged jet, Fermions emitted transverse direction from the boost direction of Z boson will be captured more than the longitudinal direction.
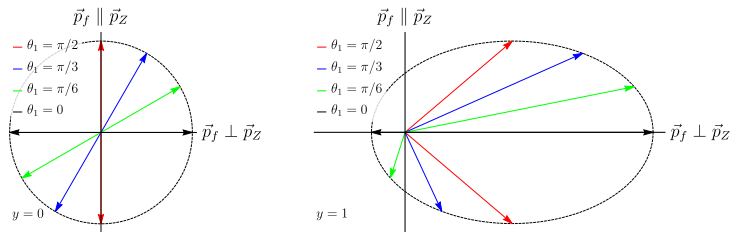
- For boosted object, phase space is beamed forward in a lab frame.

## Relativistic Aberration and angular separation of $f\bar{f}$

When we try to capture two $q\bar{q}$ by a single merged jet, Fermions emitted transverse direction from the boost direction of Z boson will be captured more than the longitudinal direction.

- For boosted object, phase space is beamed forward in a lab frame.
- For $Z \to f\bar{f}$, transverse direction is more collimated than the longitudinal direction.

Relativistic Aberration and angular separation of $f\bar{f}$

When we try to capture two $q\bar{q}$ by a single merged jet, Fermions emitted transverse direction from the boost direction of Z boson will be captured more than the longitudinal direction.


- For boosted object, phase space is beamed forward in a lab frame.
- For $Z \rightarrow f\bar{f}$, transverse direction is more collimated than the longitudinal direction.
- ME interference term is also maximized in transverse direction, and hence, we expect that we are not lose signal sensitivity much. Using merged jet is still effective for analysing CP property of S.

Distribution of ϕ

- The key signature for identifying CP state of S is angle ϕ between decay plane of Z bosons.
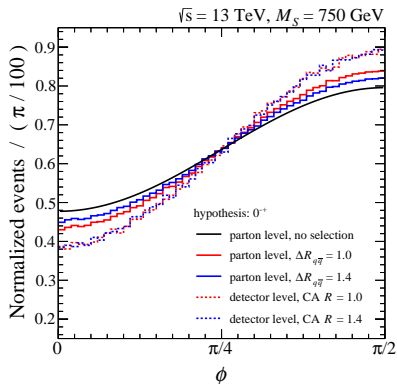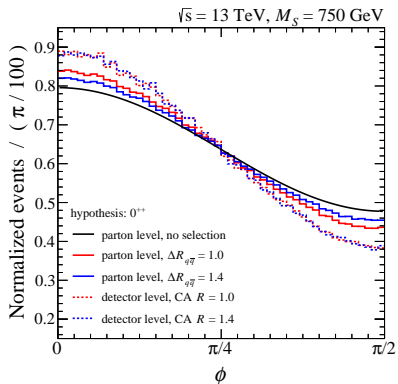
- We can reliably observe interference pattern in ϕ distribution using subjet information!

12 / 16
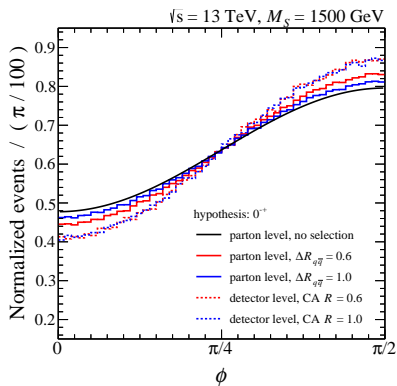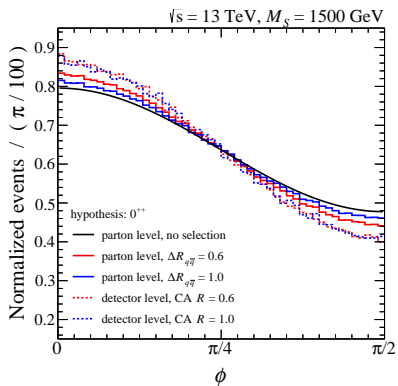
Distribution of ϕ

- Observation: interference pattern is enhanced comparing from parton information to reconstruced events
- caution: above distribution is a <u>normalized</u> distribution. Overall amplitude of interference pattern is reduced in reconstruction level due to selection efficiency.

13 / 16

Phase space restriction from jet substructure observable

- The symmetric p_T selection also gives a strong $\Delta R_{q\bar{q}}$ selection.

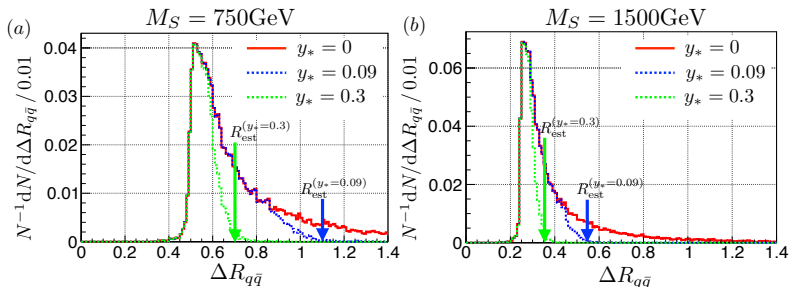$$\frac{\min(p_{T,j_1}^2, p_{T,j_2}^2)}{m_j^2}(\Delta R_{j_1 j_2})^2 > y_{\text{cut}} \tag{6}$$
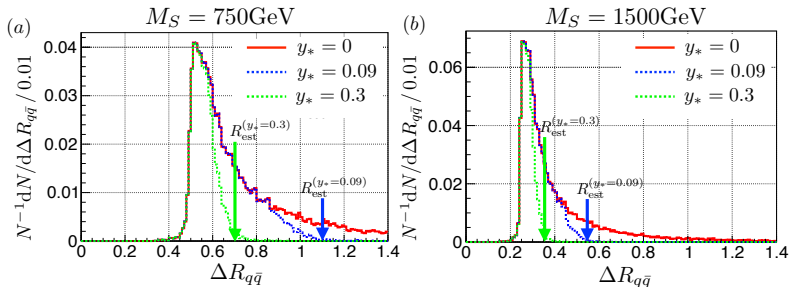
- Recall our jet definition: Cambridge-Aachen algorithm with large radius $R = 1.2$ for $m_S = 750$ GeV and $R = 0.8$ for $m_S = 1500$ GeV

Phase space restriction from jet substructure observable

- The symmetric p_T selection also gives a strong $\Delta R_{q\bar{q}}$ selection.

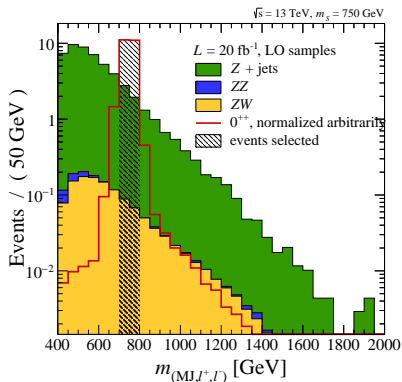$$\Delta R_{j_1 j_2} < \frac{1 + y_{\text{cut}}}{\sqrt{y_{\text{cut}}}} \frac{m_j}{p_{T,j}} \tag{6}$$

- Recall our jet definition: Cambridge-Aachen algorithm with large radius
  $R = 1.2$ for $m_S = 750$ GeV and $R = 0.8$ for $m_S = 1500$ GeV
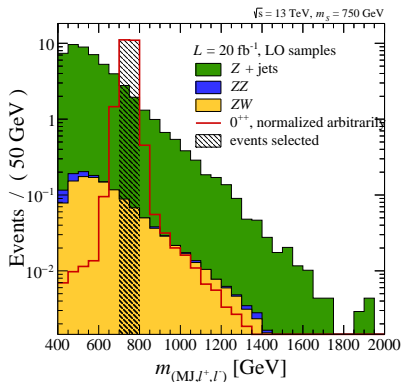
Analysis with background

In order to quantify the difference between CP even and CP odd scalar, we performed statistical analysis (matrix element method).

- QCD :
  $Z(\rightarrow \ell^- \ell^+) + \text{jets(fake } Z)$
- EW :
  $Z(\rightarrow \ell^- \ell^+) + V (\rightarrow q\bar{q})$

15 / 16

Analysis with background

In order to quantify the difference between CP even and CP odd scalar, we performed statistical analysis (matrix element method).

- QCD :
  $Z(\to \ell^- \ell^+)$ + jets(fake Z)
- EW :
  $Z(\to \ell^- \ell^+) + V (\to q\bar{q})$
- Z+jets is dominant background because of large cross section.

Analysis with background

In order to quantify the difference between CP even and CP odd scalar, we performed statistical analysis (matrix element method).
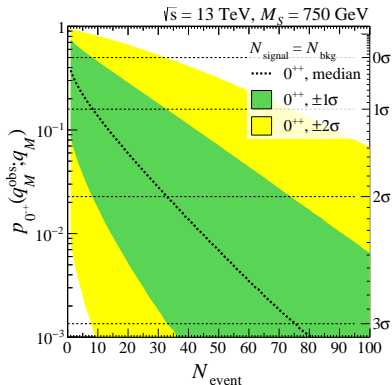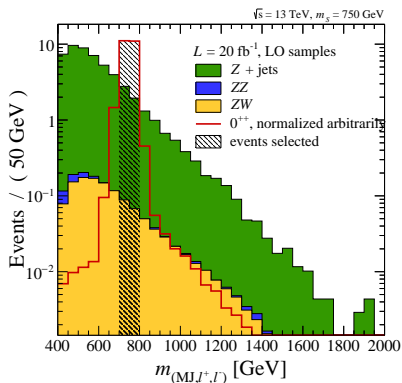
Jet substructure analysis is effective for distingushing CP even and CP odd hypothesis!

15 / 16

Conclusion

- Boosted object analysis is necessary in order to understand spin and CP nature of heavy intermediate resonance S in $S \to ZZ \to llqq$ channel.
- Merged jet analysis with jet substructure effectively select most sensitive region for identifying CP property of S.
- In kinematic phase space selection, jet substructure relying on angular information is competing with radius in jet definition. Hence the parameter should be chosen cautiously.

Backups

Cut flow	selection	750 GeV	1500 GeV
parton level		100.0 %	100.0 %
object tagging	one merged jet, two ℓ	61.0 %	63.4 %
lepton P_T	$P_T > 25$ GeV	52.0 %	58.8 %
$m_{(\ell^+, \ell^-)}$	[83, 99] GeV	47.4 %	53.5 %
m_{MJ}	[75, 105] GeV	20.6 %	25.5 %
y_{ZZ}	$|y_{ZZ}| < 0.15$	16.3 %	21.3 %
$P_{T(\mathrm{MJ})}$	$P_{T(\mathrm{MJ})} > 0.4\, m_{(\mathrm{MJ},\, \ell^+,\, \ell^-)}$	11.5 %	14.7 %
$m_{(\mathrm{MJ},\, \ell^+,\, \ell^-)}$	within $M_S \pm 50$ GeV	10.4 %	-
	within $M_S \pm 100$ GeV	-	13.4 %

Event selection criterion

		BP1 ($M_S = 750$ GeV)		
cut flow	selection criterion	$\sigma_{Z+\text{jets}}$	σ_{ZZ}	σ_{ZW}
parton level	P_T of leading jet ≥ 150 GeV	8.65 pb	8.19 fb	8.96 fb
object tagging	One merged jet, two ℓ	44.11%	55.30%	55.83%
lepton P_T	$P_T > 25$ GeV	33.47%	44.88%	47.24%
$m_{(\ell^+, \ell^-)}$	[83, 99] GeV	30.54%	40.91%	42.92%
m_{MJ}	[75, 105] GeV	1.60%	12.10%	10.72%
y_{ZZ}	$|y_{ZZ}| < 0.15$	0.72%	11.06%	9.83%
$P_{T(\text{MJ})}$	$P_{T(\text{MJ})} > 0.4\, m_{(\text{MJ}, \ell^+, \ell^-)}$	0.48%	7.22%	5.29%
$m_{(\text{MJ}, \ell^+, \ell^-)}$	within $M_S \pm 50$ GeV	0.037%	0.82%	0.68%
Cross section (σ)	-		3.16 fb	0.0671 fb	0.0609 fb

Matrix element methods

- We deployed a matrix element method in order to maximize discrimination power.
- Neyman-Pearson lemma says: likelihood ratio test is the most powerful test.
- At the parton level, we can find out the analytic form of probability from the theory as well as the likelihood functions for the hypothesis test. At the leading order, the probability density function is

$$f(\{p\}|0^{\pm}) = \frac{1}{N_{0^{\pm}}} \int dx_1 \int dx_2 f_g(x_1) f_g(x_2) |\mathcal{M}_{gg \to S \to q\bar{q}\ell^-\ell^+}(\{p\}|0^{\pm+})|^2$$

- Since S is a scalar, we can factorize the matrix element in a narrow width limit.

$$f(\{p\}|0^{\pm}) = \frac{1}{N'_{0^{\pm}}} \int dx_1 \int dx_2 f_g(x_1) f_g(x_2)$$
$$|\mathcal{M}_{gg \to S}(\{p\}|0^{\pm+})|^2 \cdot |\mathcal{M}_{S \to q\bar{q}\ell^-\ell^+}(\{p\}|0^{\pm+})|^2$$

- The likelihood ratio can be simplified if we assume

$$\frac{1}{N'_{0^{\pm+}}} \int dx_1 \int dx_2 f_g(x_1) f_g(x_2) |\mathcal{M}_{gg \to S}(\{p\}|0^{\pm+})|^2 \tag{7}$$

are identical for 0^{++} and 0^{-+}. The likelihood ratio can be written in terms of matrix element of the decay only.

$$\frac{f(\{p\}|0^{++})}{f(\{p\}|0^{-+})} = \frac{|\mathcal{M}_{S \to q\bar{q}\ell^-\ell^+}(\{p\}|0^{++})|^2}{|\mathcal{M}_{S \to q\bar{q}\ell^-\ell^+}(\{p\}|0^{-+})|^2} \tag{8}$$

- We further symmetrize momenta of quarks since q and $\bar{q}$ are indistingushable at LHC. Then, we define a loglikelihood ratio

$$q_\mathcal{M} = \sum_i^N \ln \frac{|\mathcal{M}(\{p\}_i|0^{++})|^2_{sym}}{|\mathcal{M}(\{p\}_i|0^{-+})|^2_{sym}} \tag{9}$$

16 / 16

Cambridge/Aachen Algorithm

Cambridge/Aachen Algorithm: a sequential clustering algorithm with a distance measure $(\Delta R)^2 = (\Delta \eta)^2 + (\Delta \phi)^2$
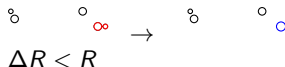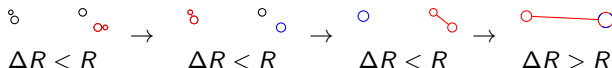
Cambridge/Aachen Algorithm: a sequential clustering algorithm with a
distance measure $(\Delta R)^2 = (\Delta \eta)^2 + (\Delta \phi)^2$

1. Check distances between objects.

Cambridge/Aachen Algorithm

Cambridge/Aachen Algorithm: a sequential clustering algorithm with a distance measure $(\Delta R)^2 = (\Delta \eta)^2 + (\Delta \phi)^2$
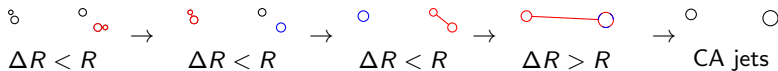
1. Check distances between objects.
2. Choose a pair of object having smallest ΔR.

Cambridge/Aachen Algorithm

Cambridge/Aachen Algorithm: a sequential clustering algorithm with a distance measure $(\Delta R)^2 = (\Delta \eta)^2 + (\Delta \phi)^2$
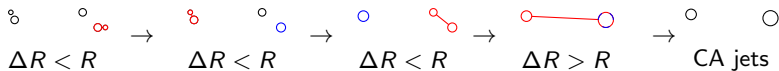
1. Check distances between objects.

2. Choose a pair of object having smallest ΔR.

3. If the two object are separated by ΔR smaller than the threshold distance R, then merge the two objects in a shortest distance by summing their momenta.

$$\circ \qquad \circ_{\circ\circ} \quad \rightarrow \quad \circ \qquad \circ_{\circ}$$
$$\Delta R < R$$

Cambridge/Aachen Algorithm

Cambridge/Aachen Algorithm: a sequential clustering algorithm with a distance measure $(\Delta R)^2 = (\Delta \eta)^2 + (\Delta \phi)^2$

1. Check distances between objects.
2. Choose a pair of object having smallest ΔR.
3. If the two object are separated by ΔR smaller than the threshold distance R, then merge the two objects in a shortest distance by summing their momenta.
4. Iterate above steps until every objects are separated by the threshold distance R.

$$\Delta R < R \qquad \rightarrow \qquad \Delta R < R \qquad \rightarrow \qquad \Delta R < R \qquad \rightarrow \qquad \Delta R > R$$

Cambridge/Aachen Algorithm

Cambridge/Aachen Algorithm: a sequential clustering algorithm with a distance measure $(\Delta R)^2 = (\Delta \eta)^2 + (\Delta \phi)^2$

1. Check distances between objects.
2. Choose a pair of object having smallest ΔR.
3. If the two object are separated by ΔR smaller than the threshold distance R, then merge the two objects in a shortest distance by summing their momenta.
4. Iterate above steps until every objects are separated by the threshold distance R.
5. Promote remaining isolated clusters as jets.

$$\Delta R < R \quad \rightarrow \quad \Delta R < R \quad \rightarrow \quad \Delta R < R \quad \rightarrow \quad \Delta R > R \quad \rightarrow \quad \text{CA jets}$$

16 / 16

Cambridge/Aachen Algorithm

Cambridge/Aachen Algorithm: a sequential clustering algorithm with a distance measure $(\Delta R)^2 = (\Delta \eta)^2 + (\Delta \phi)^2$

1. Check distances between objects.

2. Choose a pair of object having smallest ΔR.

3. If the two object are separated by ΔR smaller than the threshold distance R, then merge the two objects in a shortest distance by summing their momenta.

4. Iterate above steps until every objects are separated by the threshold distance R.

5. Promote remaining isolated clusters as jets.

$$\Delta R < R \quad \rightarrow \quad \Delta R < R \quad \rightarrow \quad \Delta R < R \quad \rightarrow \quad \Delta R > R \quad \rightarrow \quad \text{CA jets}$$

CA algorithm clusters objects in an order of increasing angle ΔR. This clustering sequence can be understood as an imitation of parton branching, and hence it has an application to a jet substructure study.

Mass drop tagger utilize clustering sequence of CA algorithm

Mass drop tagger utilize clustering sequence of CA algorithm
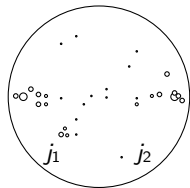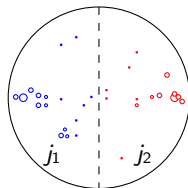
Mass drop tagger and filtering

Mass drop tagger utilize clustering sequence of CA algorithm

1. Rewind clustering of a jet j. Label two subjets as j_1 and j_2 with $m_{j_1} > m_{j_2}$.
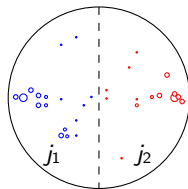
Mass drop tagger and filtering

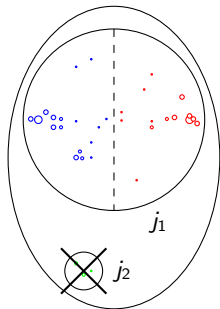Mass drop tagger utilize clustering sequence of CA algorithm

1. Rewind clustering of a jet j. Label two subjets as j_1 and j_2 with $m_{j_1} > m_{j_2}$.
2. Mass drop can happen if rewinding clustering divides j into subjets originated from light quarks.

$$m_{j_1} < \mu m_j \qquad (10)$$

Mass drop tagger and filtering

Mass drop tagger utilize clustering sequence of CA algorithm

1. Rewind clustering of a jet j. Label two subjets as j_1 and j_2 with $m_{j_1} > m_{j_2}$.

2. Mass drop can happen if rewinding clustering divides j into subjets originated from light quarks.

$$m_{j_1} < \mu m_j \qquad (10)$$

3. p_T of jets are not too asymmetric

$$\frac{\min(p_{T,j_1}^2, p_{T,j_2}^2)}{m_j^2}(\Delta R_{j_1 j_2})^2 > y_{\mathrm{cut}} \qquad (11)$$

16 / 16

Mass drop tagger and filtering

Mass drop tagger utilize clustering sequence of CA algorithm

1. Rewind clustering of a jet j. Label two subjets as j_1 and j_2 with $m_{j_1} > m_{j_2}$.

2. Mass drop can happen if rewinding clustering divides j into subjets originated from light quarks.

$$m_{j_1} < \mu m_j \qquad (10)$$

3. p_T of jets are not too asymmetric

$$\frac{\min(p_{T,j_1}^2, p_{T,j_2}^2)}{m_j^2}(\Delta R_{j_1 j_2})^2 > y_{\text{cut}} \qquad (11)$$

4. If mass drop and p_T asymmetry is not satisfied, repeat above procedure again for j_1.

Mass drop tagger and filtering

Mass drop tagger utilize clustering sequence of CA algorithm

1. Rewind clustering of a jet j. Label two subjets as j_1 and j_2 with $m_{j_1} > m_{j_2}$.

2. Mass drop can happen if rewinding clustering divides j into subjets originated from light quarks.

$$m_{j_1} < \mu m_j \qquad (10)$$

3. p_T of jets are not too asymmetric

$$\frac{\min(p_{T,j_1}^2, p_{T,j_2}^2)}{m_j^2}(\Delta R_{j_1 j_2})^2 > y_{\mathrm{cut}} \qquad (11)$$

4. If mass drop and p_T asymmetry is not satisfied, repeat above procedure again for j_1.

16 / 16

Mass drop tagger utilize clustering sequence of CA algorithm

1. Rewind clustering of a jet j. Label two subjets as j_1 and j_2 with $m_{j_1} > m_{j_2}$.

2. Mass drop can happen if rewinding clustering divides j into subjets originated from light quarks.

$$m_{j_1} < \mu m_j \tag{10}$$

3. p_T of jets are not too asymmetric

$$\frac{\min(p_{T,j_1}^2, p_{T,j_2}^2)}{m_j^2}(\Delta R_{j_1 j_2})^2 > y_{\text{cut}} \tag{11}$$

4. If mass drop and p_T asymmetry is not satisfied, repeat above procedure again for j_1.

By finding mass-dropped clusters, we can find a relevant angular scale $R_{q\bar{q}}$ to resolve $Z \to q\bar{q}$.
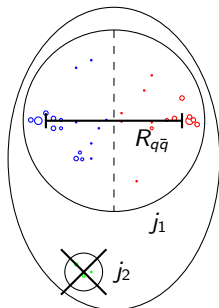
Mass drop tagger and filtering

Problem: Jets clustered with large angular scale is easily degraded by other QCD radiations.

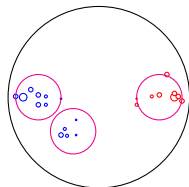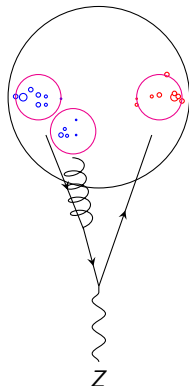$$m_q^2 = E_q^2 - |\vec{p}_q|^2 \ll E_q^2, |\vec{p}_q|^2 : \text{fine-tuned} \tag{12}$$

Mass drop tagger and filtering

Problem: Jets clustered with large angular scale is easily degraded by other QCD radiations.

$$m_q^2 = E_q^2 - |\vec{p}_q|^2 \ll E_q^2, |\vec{p}_q|^2 : \text{fine-tuned} \tag{12}$$
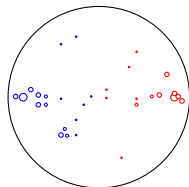
Filtering:

Mass drop tagger and filtering

Problem: Jets clustered with large angular scale is easily degraded by other QCD radiations.

$$m_q^2 = E_q^2 - |\vec{p}_q|^2 \ll E_q^2, |\vec{p}_q|^2 : \text{fine-tuned} \qquad (12)$$

Filtering:

1. Recluster jet constituent by more finer angular scale R_{filt}
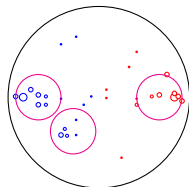
$$R_{\text{filt}} = \min\left(0.3, \frac{R_{q\bar{q}}}{2}\right) \qquad (13)$$

Mass drop tagger and filtering

Problem: Jets clustered with large angular scale is easily degraded by other QCD radiations.

$$m_q^2 = E_q^2 - |\vec{p}_q|^2 \ll E_q^2, |\vec{p}_q|^2 : \text{fine-tuned} \tag{12}$$

Filtering:

1. Recluster jet constituent by more finer angular scale R_{filt}

$$R_{\text{filt}} = \min\left(0.3, \frac{R_{q\bar{q}}}{2}\right) \tag{13}$$

2. Take n_{filt} hardest subjets and discard others.

Mass drop tagger and filtering

Problem: Jets clustered with large angular scale is easily degraded by other QCD radiations.

$$m_q^2 = E_q^2 - |\vec{p}_q|^2 \ll E_q^2, |\vec{p}_q|^2 : \text{fine-tuned} \tag{12}$$

Filtering:

1. Recluster jet constituent by more finer angular scale R_{filt}

$$R_{\text{filt}} = \min\left(0.3, \frac{R_{q\bar{q}}}{2}\right) \tag{13}$$

2. Take n_{filt} hardest subjets and discard others.

3. $n_{\text{filt}} = 3$ is often chosen to catch an $\mathcal{O}(\alpha_S)$ radiation.


Z

Mass drop tagger and filtering

Problem: Jets clustered with large angular scale is easily degraded by other QCD radiations.

$$m_q^2 = E_q^2 - |\vec{p}_q|^2 \ll E_q^2, |\vec{p}_q|^2 : \text{fine-tuned} \tag{12}$$

Filtering:

1. Recluster jet constituent by more finer angular scale R_{filt}

$$R_{\text{filt}} = \min\left(0.3, \frac{R_{q\bar{q}}}{2}\right) \tag{13}$$

2. Take n_{filt} hardest subjets and discard others.

3. $n_{\text{filt}} = 3$ is often chosen to catch an $\mathcal{O}(\alpha_S)$ radiation.

After then, we merged most soft filtered subjet into its nearest subjet in ΔR.
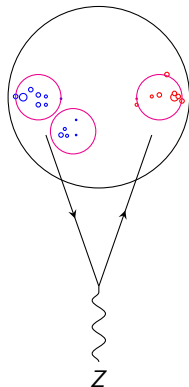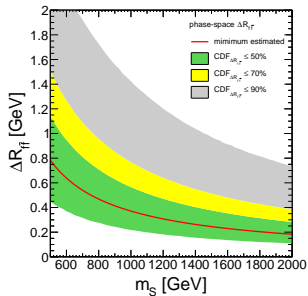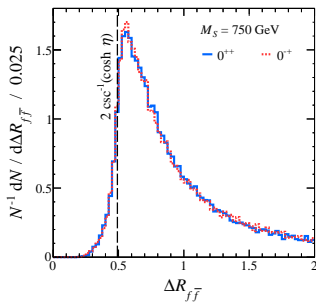
Z
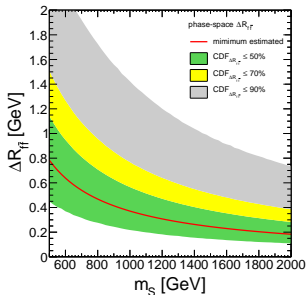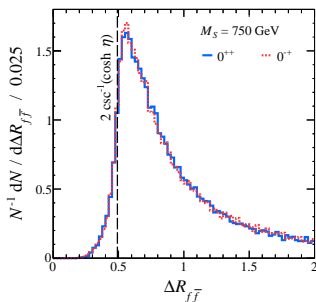
Collimated Fermions from boosted Z boson decay

- As the mass gap between S and Z becomes larger, the angular separation of Fermions are getting smaller.
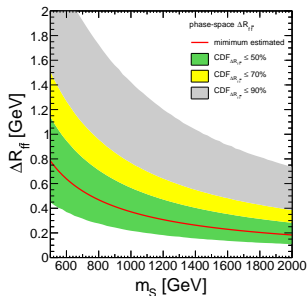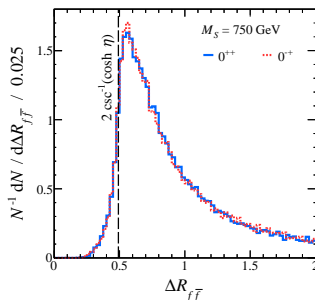
- As the mass gap between S and Z becomes larger, the angular separation of Fermions are getting smaller.
- For $m_S = 750 \text{ GeV}$, intermediate region between resolved and collimated
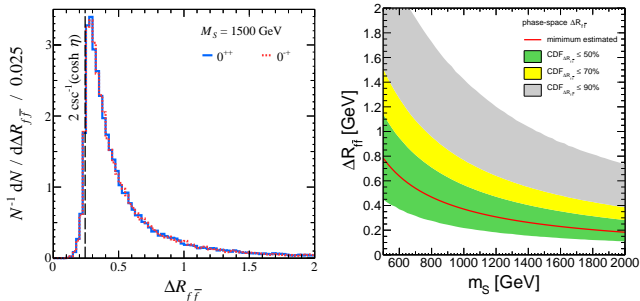
$$\Delta R_{f\bar{f}} \gtrsim 0.5 \tag{14}$$

$$(\Delta R_{f\bar{f}})^2 = (\Delta \eta)^2 + (\Delta \phi)^2 \gtrsim \left(\frac{2m_Z}{p_{T,Z}}\right)^2 \tag{15}$$
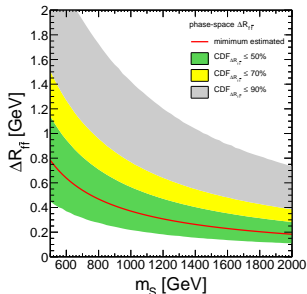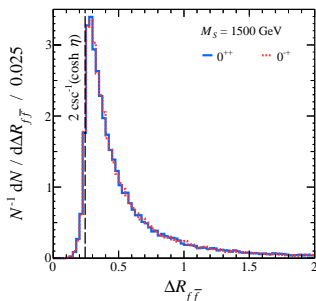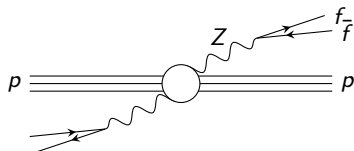
Collimated Fermions from boosted Z boson decay
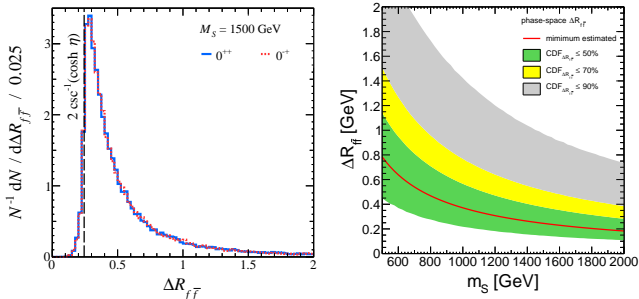
- As the mass gap between S and Z becomes larger, the angular separation of Fermions are getting smaller.
- For $m_S = 1500 \ \mathrm{GeV}$, collimated

$$\Delta R_{f\bar{f}} \gtrsim 0.3 \tag{14}$$

$$(\Delta R_{f\bar{f}})^2 = (\Delta\eta)^2 + (\Delta\phi)^2 \gtrsim \left(\frac{2m_Z}{p_{T,Z}}\right)^2 \tag{15}$$

- As the mass gap between S and Z becomes larger, the angular separation of Fermions are getting smaller.
- Q: Is boosted object analysis effective for studying properties (such as spin and CP) of the resonance S?

- As the mass gap between S and Z becomes larger, the angular separation of Fermions are getting smaller.
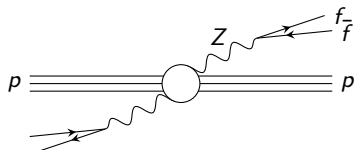- Q: Is boosted object analysis effective for studying properties (such as spin and CP) of the resonance S?
- We will see that boosted object analysis is necessary in order to maximize the discrimination power for determining spin and CP of S.

Angular separation of particles from Z boson decay

Lorentz invariant angular separtion under a boost along the beam direction

$$(\Delta R)^2 = (\Delta \eta)^2 + (\Delta \phi)^2 \approx \frac{m_Z^2}{p_{T,f} \, p_{T,\bar{f}}} \tag{14}$$

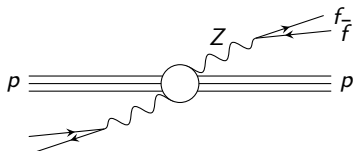## Angular separation of particles from Z boson decay

Lorentz invariant angular separtion under a boost along the beam direction

$$(\Delta R)^2 = (\Delta \eta)^2 + (\Delta \phi)^2 \approx \frac{m_Z^2}{p_{T,f} p_{T,\bar{f}}} \tag{14}$$

ΔR is from inner product between p_f^μ and $p_{\bar{f}}^\nu$. For massless f,

$$\eta_{\mu\nu} p_f^\mu p_{\bar{f}}^\nu = p_{T,f} p_{T,\bar{f}}(\cosh \Delta \eta - \cos \Delta \phi) \tag{15}$$

$$\cosh \Delta \eta - \cos \Delta \phi = \frac{\eta_{\mu\nu} p_f^\mu p_{\bar{f}}^\nu}{p_{T,f} p_{T,\bar{f}}} = \frac{m_Z^2}{2 p_{T,f} p_{T,\bar{f}}} \tag{16}$$

Lorentz invariant angular separation under a boost along the beam direction

$$(\Delta R)^2 = (\Delta \eta)^2 + (\Delta \phi)^2 \approx \frac{m_Z^2}{p_{T,f} p_{T,\bar{f}}} \tag{14}$$

ΔR is from inner product between p_f^μ and $p_{\bar{f}}^\nu$. For massless f,
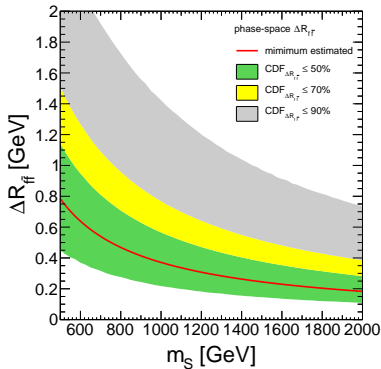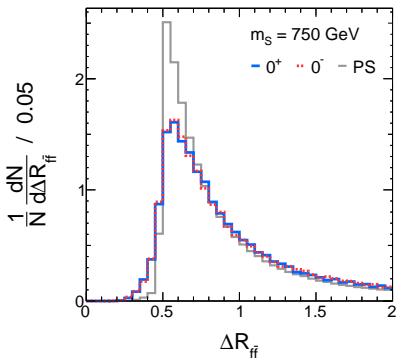
$$\eta_{\mu\nu} p_f^\mu p_{\bar{f}}^\nu = p_{T,f} p_{T,\bar{f}} (\cosh \Delta \eta - \cos \Delta \phi) \tag{15}$$

$$\cosh \Delta \eta - \cos \Delta \phi = \frac{\eta_{\mu\nu} p_f^\mu p_{\bar{f}}^\nu}{p_{T,f} p_{T,\bar{f}}} = \frac{m_Z^2}{2 p_{T,f} p_{T,\bar{f}}} \tag{16}$$

In terms of $p_{T,Z}$ we can rewrite ΔR by

$$(\Delta R)^2 = (\Delta \eta)^2 + (\Delta \phi)^2 \approx \frac{1}{z(1-z)} \frac{m_Z^2}{p_{T,Z}^2}, \quad z(1-z) = \frac{p_{T,f} p_{T,\bar{f}}}{p_{T,Z}^2} \tag{17}$$

$$(\Delta R)^2 \approx \frac{1}{z(1-z)} \frac{m_Z^2}{p_{T,Z}^2} \geq \left(\frac{2m_Z}{p_{T,Z}}\right)^2 \tag{18}$$

For $m_S = 750 \ \mathrm{GeV}$ resonance, $\Delta R \gtrsim 0.5$. For electron (jet) isolation in reconstruction level, we often set an isolation angular scale 0.3 (0.4).